



Early-Oil Generation Potential of Type II-S Kerogen in the Upper Cretaceous (Cenomanian–Turonian) Organic-Rich Carbonate Succession from Ajloun Region in Northern Jordan

Mohammed Hail Hakimi¹ · Mohammad Alqudah² · Khairul Azlan Mustapha³ · Mikhail A. Varfolomeev¹ · Aref Lashin⁴ · Baleid Ali Hatem³ · Afkiah Rahim⁵ · Souvik Sen⁶ · Ahmed E. Radwan⁷ · Nura Abdulmumini Yelwa^{3,8}

Received: 11 June 2022 / Accepted: 24 August 2022 / Published online: 28 September 2022
© King Fahd University of Petroleum & Minerals 2022

Abstract

This study examines the geochemical and petrological characteristics of 16 carbonate-rich (i.e., chalky marl, chalky limestone, and limestone) samples of the Upper Cretaceous Shu'ayb Formation in the Ajloun region, northern Jordan, to decipher the organic matter characteristics and predict the geological temperatures for oil generation. The carbonate-rich sediments under investigation exhibit high TOC (up to 12.39 wt%) and high hydrogen index (314–920 mg HC/g TOC), indicating Types I-II kerogens. The dominance of such hydrogen-rich kerogen is confirmed by the fluorescent alginite, amorphous organic matter (AOM), and bituminite organic matter. The studied organic facies are sulfur-rich and comprise of Type II organic matter, exhibiting the possibility of producing paraffinic oil with a low wax component, according to pyrolysis–gas chromatography. The broad distributions of activation energy (37–66 kcal/mol) in the bulk kinetic model of the analyzed samples show a mixture of organic matter (i.e., mainly marine-derived organic matter and minor land plant input).

The kinetic models suggest that bulk petroleum formation began at relatively low geological temperatures between 104 and 116 °C, which corresponds to a vitrinite reflectance range of 0.58–0.66%. These activation energy distributions and low anticipated vitrinite reflectance values are largely compatible with the Type II-S kerogen organic facies, suggesting that the investigated Upper Cretaceous organic-rich carbonate may have produced sulfur-rich oils during the initial phases of kerogen conversion.

Keywords Upper Cretaceous · Organic-rich carbonates · Hydrogen-rich kerogen · Kinetics modeling · Wadi Ajloun · Northern Jordan

1 Introduction

Organic matter-rich formations are the key hydrocarbon resources worldwide. The study of the organic properties and petroleum generative potential shed critical insights on the conventional as well as unconventional petroleum resource potential. Geochemical and microscopic investigations are the primary tools to achieve these objectives [1].

Jordan ranks eighth out of 37 countries in the world with resources of organic-rich sediment, exceeding 65 billion tons of oil shale deposits [2]. Upper Cretaceous-Eocene sediments across Jordanian basins host a number of organic matter-rich

✉ Mohammed Hail Hakimi
ibnalhakimi@yahoo.com

¹ Department of Petroleum Engineering, Kazan Federal University, Kazan, Russia420008

² Department of Earth and Environmental Sciences, Yarmouk University, Shafeeq Irshaidat Street, Irbid 21163, Jordan

³ Department of Geology, University of Malaya, 50603 Kuala Lumpur, Malaysia

⁴ College of Engineering-Petroleum and Natural Gas Engineering Department, King Saud University, Riyadh 11421, Saudi Arabia

⁵ Faculty of Engineering, School of Civil Engineering, Universiti Teknologi Malaysia, Johor, Malaysia

⁶ Dynasty Building, Geologix Limited, Wing A, Level 4 Andheri Kurla Road, Andheri (E), Mumbai, Maharashtra 400059, India

⁷ Institute of Geological Sciences, Jagiellonian University, Gronostajowa 3a, 30-387 Kraków, Poland

⁸ Department of Geology, Usmanu Danfodiyo University, Sokoto PMB 2346, Nigeria



strata, such as bituminous carbonates, marls, chalky marles, and chalks [3]. All of these oil resources are considered to be of high quality [4–7].

A number of researchers have assessed the origin, paleo-depositional, climatic, and geochemical circumstances of organic matter, as well as the potential for petroleum generation potential of these sediments based on geochemical analyses and microscopic investigations [8–12]. Most of the Upper Cretaceous and Eocene sediments in Jordan's central and northern areas are organic-rich with high TOC content (up to 10 wt%). These were deposited in marine anoxic environments and received considerable alginite materials [13–15]. While Hakimi et al. [3, 6] reported the occurrence of a variety of organic materials within the Maastrichtian oil-shales recovered from the northern and central Jordan, little is known about the organic-rich sediments found in the Upper Cretaceous successions of northern Jordan, especially those from the Cenomanian–Turonian ages, which is the primary objective of this study.

The current research focuses on the Upper Cretaceous organic-rich carbonates (Cenomanian–Turonian), particularly those of the Shu'ayb Formation in the Ajloun area in northern Jordan (Fig. 1). Multi-geochemical methods and microscopic investigations are combined to characterize the organic matter and determine its petroleum generative potential. Additionally, this study discusses the utility of bulk kinetic results to predict maximum geological temperatures for oil generation.

2 Geological Setting

Major shifts in the depositional environment associated with changes in the tectonic setting of the north-western margin of the Arabian Plate marked the Cenomanian in Jordan. These shifts are recognized by changes in the type of sediment deposited during that time [16]. At the Cenomanian–Turonian boundary, organic matter-rich sediments were deposited in the Wades Mujib and Ajloun sites. The studied Cenomanian–Turonian sediments represent inner and mid-shelf [17] which overlie the shallow sub-tidal and supra-tidal platform sediments of the Cenomanian age [18, 19].

The Wadi Ajloun area in the northern part of Jordan is filled with Upper Cretaceous rocks, ranging from Cenomanian to Turonian in age (Fig. 2). The Upper Cretaceous rock units are known as the Ajloun group [20]. The group comprises several formations listed from oldest to youngest as follows: (1) Fuhays, (2) Hummar, and (3) Shu'ayb (Fig. 1B). The Ajloun sediments primarily consist of soft marl, marly limestone, and shale with thinner and harder interbedded limestone [20]. The Fuhays Formation was deposited in the early Cenomanian and consists primarily of marly sediments [21]. This formation underlies the upper Cenomanian Hum-

mar Formation, which mainly consists of hard to massive dolomitic limestone and some intercalations of softer, marly to chalky beds [21].

The Shu'ayb Formation overlies the Hummar Formation. It contains primarily carbonate sediments, including chalks (gray/white colored), chalky limestones, and organic-rich chalky marls (mostly dark gray colored) which were deposited during the late Cenomanian to the early Turonian ages [21]. These carbonates are organic matter-rich, exposed in Ajloun area (Fig. 2) and are the main zones of interest for this study. The limestone-dominated Turonian Wadi AS Sir Formation is the uppermost formation of the Ajloun Group (Fig. 1B).

3 Materials and Experimental Methods

In this study, 16 rock samples of organic-rich carbonates (i.e., chalky marl, chalky limestone, and limestone) were collected from the Upper Cretaceous (Cenomanian–Turonian) Shu'ayb Formation that outcrops at the Ajloun area of northern Jordan (Fig. 2). Before geochemical and petrological studies, weathered surfaces of the samples were removed.

Polished sample blocks were investigated under the microscope for the identification of organic facies [22]. In this case, entire samples were broken into small pieces (about 1–2 mm, pea sized) and implanted into molds employing a SeriFix resin with cold-mount hardener combination. After being hardened, the blocks were crushed to expose the sample surfaces. Then, these were singly polished to smoothen the surfaces with the aid of silicon carbide paper and alumina powder. Initially, the grade was 1 mm; then, a 0.05-mm grade was utilized with isopropyl alcohol as the lubricant. The polished blocks then underwent oil immersion and were examined under plane-polarized reflected white light and cross-polarized UV light utilizing a LEICA DM6000M microscope coupled with fluorescence illuminators.

For the geochemical evaluation, the inorganic carbonate content was eliminated from pulverized samples (<200 mesh) after treatment with 10% HCl solution. Bulk pyrolysis (Rock-Eval), TOC, and pyrolysis–gas chromatogram (Py–GC) analyses were performed on the treated samples along with bulk kinetic modeling. TOC (weight percent) was determined using a LECO CS244 analyzer.

Bulk pyrolysis was carried out on ten selected powdered samples using a source rock analyzer (SRA) in accordance with the techniques specified by Espitalie et al. [23] and Lafargue et al. [24]. From these analyses, the maximum temperature for S₂ production (T_{max}), the amount of free hydrocarbons prior to pyrolysis (S₁) and post-pyrolysis residual hydrocarbons (S₂) were obtained. In addition, the hydrogen index (HI), production index (PI) and hydrocar-

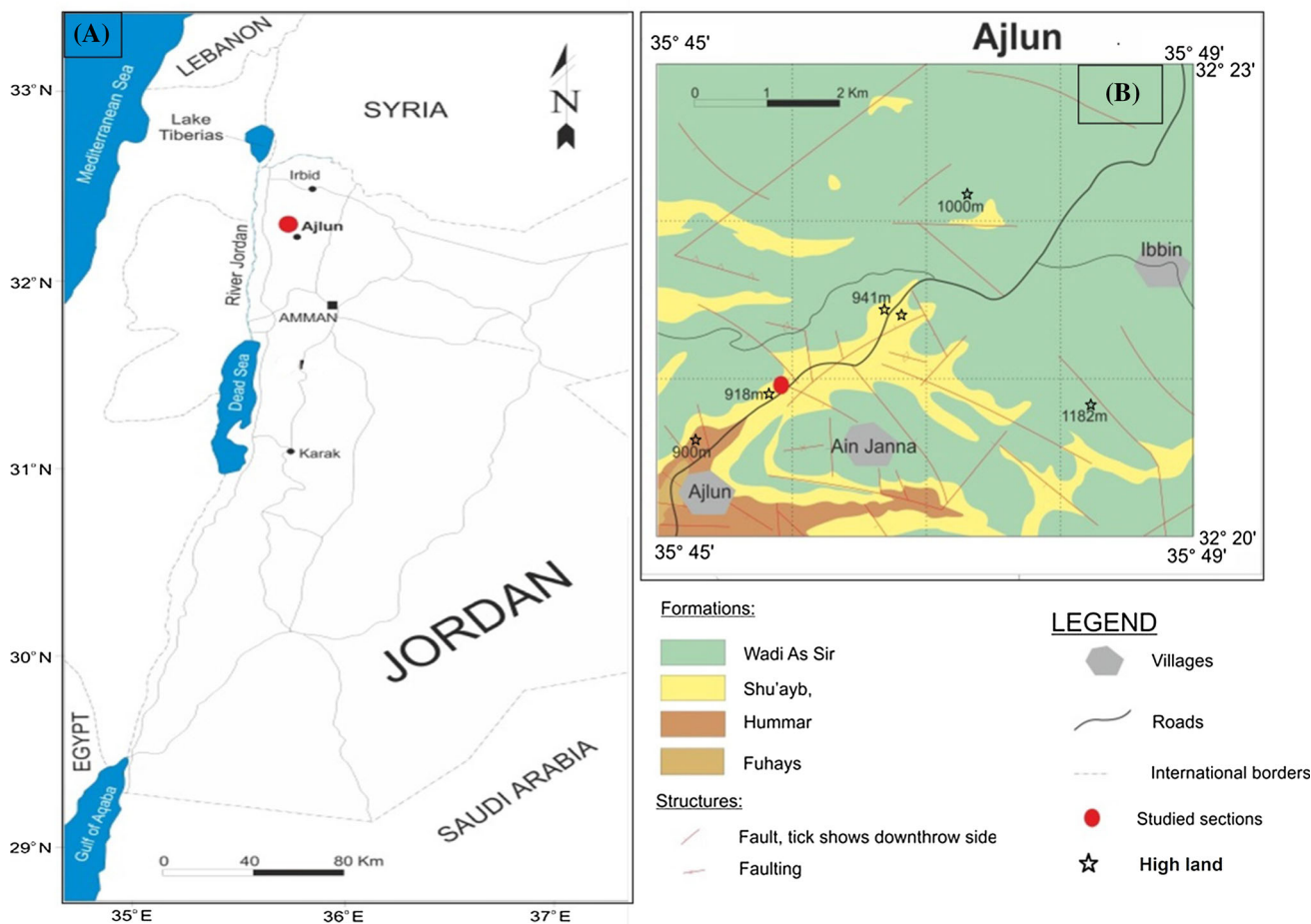


Fig. 1 Geographic maps of **A** the Wadi Ajloun area in northern Jordan, and **B** the studied area showing the geological exposures of various formations

bon potential (PY) were also determined utilizing the TOC and bulk pyrolysis data [25–27].

Ten samples were selected for bitumen extraction. Samples (20–25 g) were Soxhlet-extracted for 72 h, with a solvent mixture comprising of 93% vol. dichloromethane and 7% vol. methanol. The sample extracts were then reserved for Py–GC and Rock–Eval assay. As outlined by Larter [28], Py–GC was utilized to decipher the chemical composition of the pyrolysates and associated kerogen properties. The Py–GC analysis was also used to determine the sulfur-rich kerogen as detected by its organic sulfur compounds (e.g., thiophenes) [29].

This test was performed using a Frontier Lab Pyrolyser, coupled to an inert quartz tube and an Ultra ALLOY-5 column (30 m X 0.25 mm) fitted into an Agilent 6890 gas chromatography (GC). The analyzed samples were flash pyrolysed at 600 °C. Within the Py–GC furnace, the compounds released

from pyrolysis were separated through column with the temperature programmed GC oven from 30 to 300 °C (at 4 °C/min rate) and then held 600 °C for 30 min. In addition to a methane peak, the chromatograms revealed a series of *n*-alkene and *n*-alkane signatures, as well as a few aromatic signatures in-between.

For modeling of bulk kinetics, five finely ground samples (20–30 mg) were selected from the 10 extracted samples and pyrolysed under non-isothermal conditions in the Weatherford SRA pyrolyzer at different rates of heating (1, 5, 10, 25 and 50 °C). The bulk petroleum formation curves recorded for each heating rate were used as input to ascertain kinetic characteristics [activation energy (Ea) distribution and the frequency factor (A)] [29, 30]. The activation energy (Ea) distribution and the frequency factor (A) were calculated using Kinetics 2000® and KMODTM® software packages [31, 32].

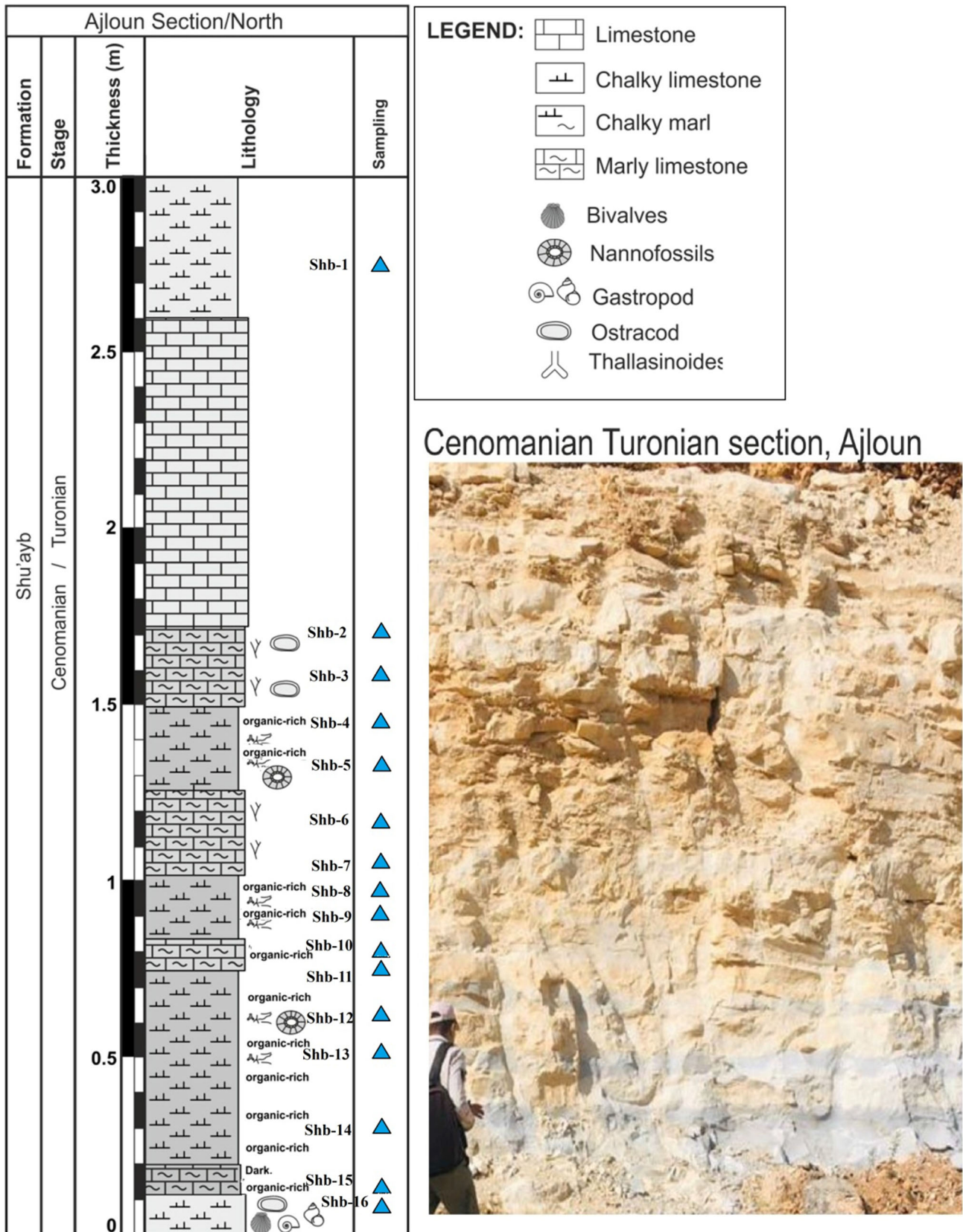


Fig. 2 Sedimentary log and field photographs of the studied Shu'ayb Formation in the study area (modified after Momani, 2021)

4 Results and Interpretations

4.1 Organic Petrography

Microscopic examinations were performed to detect the kerogens in the investigated organic-rich carbonates. The results exhibit that these samples dominantly comprise carbonate minerals, and host liptinite macerals, as depicted in the microphotographs of Fig. 3. The occurrence of kerogen assemblages and their characteristics were evaluated using UV radiation and plane-polarized reflected white light (Fig. 3). Liptinite macerals dominated all of the samples. These macerals appeared brown-dark brown under reflected white light (Fig. 3a and b). The fluorescence intensities vary from yellow to greenish-yellow when exposed to UV light (Fig. 3c–f). UV radiation was primarily used to distinguish the morphology and structure of liptinite assemblages. In this case, most of the examined samples showed structured and unstructured macerals, including alginite, amorphous organic matter (AOM), and bituminite (Fig. 3a–h). Alginite occurs in two forms: lamalginite and telalginite (Fig. 3b, e), both of which are thought to have been formed in a marine environment.

Researchers indicated an anoxic bottom water environment for the accumulations of such alginites [3, 22]. We also observed telalginite and lamalginite assemblages which indicate the presence of tasmanite algae (Fig. 3f). In addition to the telalginite and lamalginite assemblages, the alginite assemblages were also infused with the mineral matrix (Fig. 3b, c). These degraded alginites are brown under white light (Fig. 3b) with a greenish-yellow fluorescence under UV light (Fig. 3c) and are classified as AOM. The AOM exhibiting fluorescence suggests that these AOMs were derived from degraded or reworked algal organic matter [33, 34].

Indigenous structureless bitumen was also observed in few cases (Fig. 3g, h), and inferred as bituminite II following Pickel et al. [35]. Under white light, these bituminites exhibit a reddish brown to light gray color (Fig. 3g) with a greenish-yellow fluorescence when exposed to UV light (Fig. 3h). A small portion of vitrinite was also found in some of the analyzed samples. This maceral is represented by brittle phytoclasts with angular surfaces, varying shapes, and dark gray color under reflected white light (Fig. 3k).

4.2 Total Organic Carbon Content

TOC content is extensively employed as an indicator of organic richness as well as hydrocarbon generation capacity upon maturity [36]. Clay-rich and carbonate-rich sediments with TOC level greater than 1% are considered to have a good hydrocarbon source potential [37]. The studied carbonate-rich samples are organically rich, as revealed by TOC ranging from 1.00 to 12.39% (Table 1 and Fig. 4a). Eight of the 16

samples have TOC < 3 wt% (1.00–2.50 wt%), whereas the rest of the samples exhibited TOC values between 3.15 and 12.30%. Consequently, the bulk of the examined organic-rich carbonates in the Upper Cretaceous (Cenomanian–Turonian) succession are inferred as good to excellent source rocks (Fig. 4A) for substantial quantities of hydrocarbon generation at optimum maturation.

4.3 Rock–Eval Pyrolysis Results

Table 1 summarizes the S_1 , S_2 , T_{max} , PI, and HI obtained by Rock Eval pyrolysis of the 10 selected samples. The hydrocarbon yields from cracking of kerogen (S_2) exhibits a range between 3.87 and 113.13 mg HC/g. We observed $S_2 > 15$ mg HC/g rock (17.29–113.13 mg HC/g rock) in almost half of the examined samples ($n = 7$) (Table 1). Three samples had lower S_2 yields (3.87–9.19 mg HC/g rock, Table 1). Based on these results, we infer that the majority of the carbonate-rich samples have good to excellent hydrocarbon generating capability (Fig. 4B). In contrast, pyrolysis findings indicate that the tested samples had minimal free hydrocarbon yields, given that S_1 values ranged from 0.03 to 1.33 mg HC/g, implying thermal immaturity.

Nevertheless, S_2 petroleum yields are likewise consistent with TOC content, resulting in high HI between 314 and 920 mg hydrocarbon/g TOC. The tested specimens may be classified into two categories based on their HI values: those having HI between 300 and 600 mg HC/g TOC (samples Shb-2, Shb-3, Shb-6, Shb-9, Shb-13 and Shb-14, Table 1) and those with HI > 600 mg HC/g TOC (samples Shb-4, Shb-8, Shb-11 and Shb-15).

During pyrolysis, the T_{max} values of all the examined samples varied from 410 to 435 °C (Table 1). Only two samples indicated highest T_{max} values in the range of 431–435 °C, while the majority of the samples had $T_{max} < 430$ °C (410–425 °C) (Table 1). The PI values acquired using Rock–Eval pyrolysis varied from 0.01 to 0.03 and were obtained in addition to the T_{max} data (Table 1). The Rock–Eval T_{max} and PI data were employed as geochemical thermal maturation indicators, which imply that the studied organic-rich carbonates of the Upper Cretaceous Shu'ayb Formation in northern Jordan's Wadi Ajloun are still immature source rocks.

4.4 Open Pyrolysis–Gas Chromatography

Py–GC provides critical insights about the composition of kerogens [38, 39]. Additionally, the potential of petroleum generation and oil quality can also be predicted from GC analysis of pyrolysate S_2 materials [39–42].

Figure 5 presents the Py–GC chromatograms of the extracted specimens. The chromatograms indicate a high abundance of the aliphatic compounds (n -alkene, n -alkane)

Table 1 Geochemical results of TOC, TS contents, bulk Rock–Eval pyrolysis and pyrolysis–gas chromatography (Py–GC) of the analyzed organic-rich carbonate rock throughout the Upper Cretaceous Shu’ayb Formation from outcrops area in Ajloun area show the organic matter characteristics and their contributions to oil generation resources in northern Jordan

Samples ID	TOC wt.%		Bulk Rock–Eval pyrolysis										Pyrolysis–gas chromatography (Py–GC)				
	Measured	Calculated	Kerogen type					Petroleum compositions									
	S ₁ (mg/g)	S ₂ (mg/g)	T _{max} (°C)	HI (mg/g)	PY (mg/g)	PI (mg/g)	2-, 3-dimethylthiophene (%)	Xylene (%)	n-C ₉ (%)	xy/C ₈ ratio	C ₁ –C ₅ (%)	C ₆ –C ₁₄ (%)	+ C ₁₅ (%)	C ₈ /xy ratio			
Shb-1	–	–	–	–	–	–	–	–	–	–	–	–	–	–			
Shb-2	0.03	3.87	435	320	3.900	0.01	44.17	16.76	39.07	0.30	49.42	37.51	13.07	3.33			
Shb-3	0.07	4.52	425	314	4.59	0.02	45.80	12.93	41.26	0.39	47.52	40.85	11.64	2.58			
Shb-4	0.51	60.29	412	802	60.8	0.01	42.25	6.63	51.12	0.13	40.48	45.96	13.56	7.92			
Shb-5	–	–	–	–	–	–	–	–	–	–	–	–	–	–			
Shb-6	0.06	5.6	431	467	5.66	0.01	43.51	6.75	49.75	0.38	56.08	31.05	12.87	2.62			
Shb-7	–	–	–	–	–	–	–	–	–	–	–	–	–	–			
Shb-8	0.75	73.4	415	650	74.15	0.01	46.79	6.79	46.41	0.31	41.72	55.27	3.01	3.22			
Shb-9	0.09	9.19	423	431	9.28	0.01	46.35	8.15	45.50	0.29	46.02	41.85	12.13	3.49			
Shb-10	–	–	–	–	–	–	–	–	–	–	–	–	–	–			
Shb-11	0.54	60.91	417	628	61.45	0.01	42.97	11.71	45.32	0.39	41.77	44.28	13.96	2.58			
Shb-12	–	–	–	–	–	–	–	–	–	–	–	–	–	–			
Shb-13	0.14	17.29	414	474	17.43	0.01	53.87	9.24	36.88	0.29	45.73	39.65	14.62	3.43			
Shb-14	0.46	34.11	421	523	34.57	0.01	49.55	8.02	42.43	0.34	42.56	53.56	3.88	2.90			
Shb-15	1.33	113.13	410	920	114.46	0.01	33.98	3.52	62.50	0.14	43.64	41.45	14.91	6.95			
Shb-16	–	–	–	–	–	–	–	–	–	–	–	–	–	–			

TOC total organic carbon, wt%, S₁ volatile hydrocarbon (HC) content, mg HC/g rock, S₂ remaining HC generative potential, mg HC/g rock, T_{max} temperature at maximum of S₂ peak, HI hydrogen index = S₂ × 100/TOC, mg HC/g TOC, PY potential yield = S₁ + S₂ (mg/g), PI production index = S₁/(S₁ + S₂)

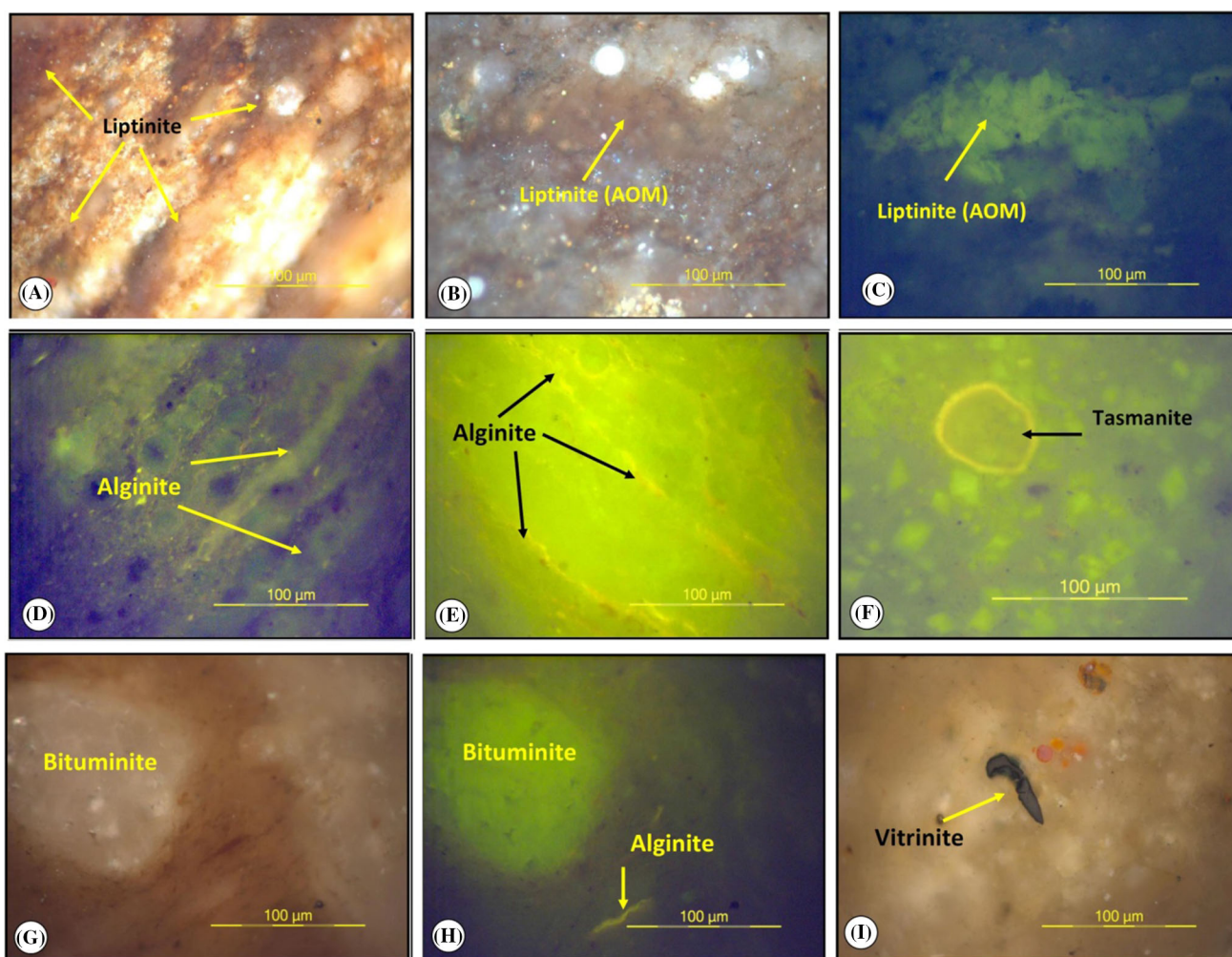


Fig. 3 Photomicrographs of the investigated organic-rich carbonates of the Upper Cretaceous Shu'ayb Formation, under reflected light, and fluorescence under UV, with a field width of 0.2 mm. **a** liptinites exhibiting brown to dark brown colors; **b, c** AOM appearing brown, with greenish-yellow fluorescence; **d-f** alginite exhibiting yellow-greenish

fluorescence, displaying *lamalginite*, *telalginite*, and *Tasmanite* forms; **g, h** light gray-colored bituminite with greenish-yellow fluorescence; and **i** vitrinite maceral with angular shapes and dark gray color under reflected white light

along with lower aromatic content. The distributions of the *n*-alkene and *n*-alkane are unimodal, with carbon numbers spanning from C₅ to beyond C₃₀. The bulk of the samples have substantial concentrations of *n*-alkene and *n*-alkane molecules in the low and high molecular carbon fractions. Toluene, xylene, and benzene alkylbenzenes are the most common aromatic hydrocarbon compounds. In addition to the aliphatic and aromatic hydrocarbons, the pyrolysates include a significant amount of sulfur-derived organic compounds (Fig. 5).

Based on the particular pyrolysate distributions of *n*-octane (C₈) and xylene (xy), we generated several ratios to decipher the kerogen types and their hydrocarbon generation potential [42, 43]. For example, oil-sourcing intervals exhibit C₈/xy ratio > 1 and it is less than 1 in the gas-prone sources.

The kerogen type, on the other hand, is defined by the proportion of xylene to *n*-octane given by the xy/C₈ index [40]. This index is divided into three categories, depending on their values. The Type I and Type II kerogens exhibit xy/C₈ usually lower than 0.4, while in combined II/III kerogens, it ranges from 0.4 to 1.3. In the type III kerogens xy/C₈ has been found to be greater than 1.3 [40].

The examined organic-rich carbonates of the Upper Cretaceous (Cenomanian–Turonian) succession yield xy/C₈ values of lower than 0.4 (0.13–0.39) (Table 1), indicating the dominance of type I and type II kerogens. Most of the samples investigated have a C₈/xy ratio of 2.58 to 7.92 (Table 1), suggesting that these carbonate-rich sediments might generate considerable quantities of oil upon reaching thermal maturity.

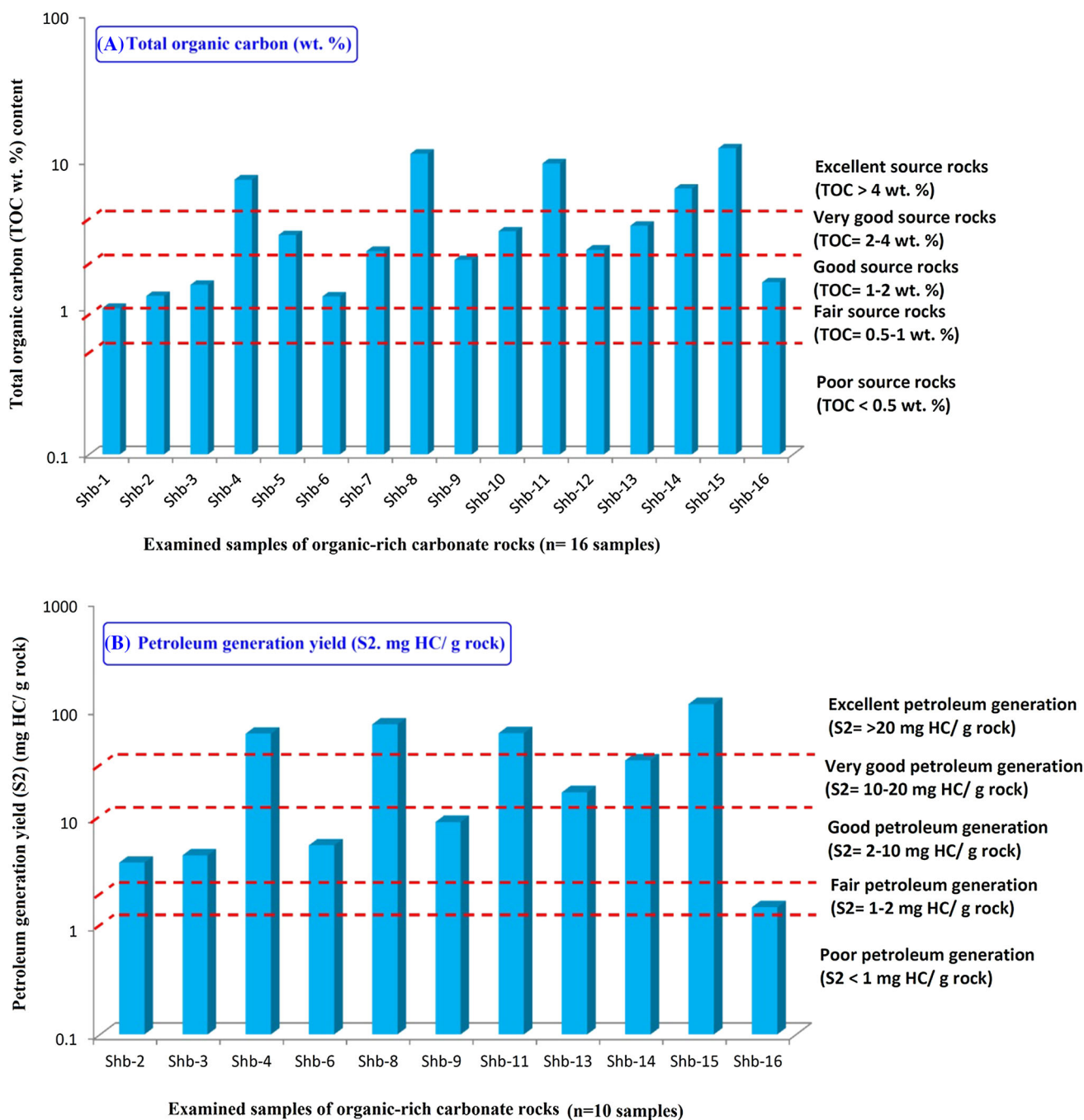


Fig. 4 Histograms of **A** the TOC (wt%) distributions in the analyzed samples, and **B** the petroleum potential yield via programmed pyrolysis, showing good-to-excellent source characteristics of the analyzed Shu'ayb carbonates

4.5 Bulk Kinetics Modeling Results

Table 2 summarizes the bulk kinetics results obtained from the selected samples of the Late Cretaceous Shu'ayb Formation and the results are presented in Fig. 6. According to the kinetic models, activation energy (E_a) distributions are broad, ranging between 37 and 66 kcal/mol, while the

frequency factor (A) varies between $1.3274E + 13/\text{sec}$ and $8.2311E + 13/\text{sec}$.

As the kerogen composition influences the bulk kinetics of petroleum generation, it is expected that the thermal stabilities and transformational behavior of each compositional group found in kerogens impact the distributions of 'Ea' and 'A' [44, 45]. The broad distribution observed in E_a values is indicative of a mixture of organic matter [6]. This

Table 2 Activation energy distributions (kcal/mol) for five selected organic-rich carbonate rocks within the Upper Cretaceous Shu’ayb Formation from outcrops area in Ajloun area, northern Jordan

Samples/AE (kcal/mol)	37	38	39	40	41	42	43	44	45	46	47	48	49	50	
Shb-3	–	–	0.37	–	0.24	0.11	0.45	–	0.82	0.14	3.56	6.23	10.96	18.26	
Shb-4	–	0.08	0.04	0.03	0.18	0.09	–	–	–	–	4.27	7.32	13.67	26.41	
Shb-8	–	–	–	0.07	0.08	0.13	0.16	0.19	0.31	–	0.38	0.34	2.45	6.49	
Shb-14	0.12	–	0.18	0.04	0.19	0.34	0.13	0.16	1.41	5.29	9.43	16.48	24.16	15.86	
Shb-15	–	–	–	–	–	0.86	–	0.58	0.61	0.74	1.25	2.15	2.98	5.72	
51	52	53	54	55	56	57	58	59	60	61	62	63	64	65	66
23.39	16.14	10.54	3.71	2.18	1.63	0.57	–	0.16	0.55	–	–	–	–	–	–
20.52	13.67	7.12	2.38	1.63	1.07	–	0.81	0.40	–	–	0.28	–	–	–	–
12.32	17.82	22.34	13.95	9.36	4.93	2.41	2.74	0.13	1.9	0.15	–	1.33	–	–	–
12.28	6.53	2.67	1.87	1.02	0.66	0.17	–	0.66	–	–	–	–	–	–	–
8.05	13.91	19.43	18.42	10.19	5.92	3.59	1.21	1.69	0.64	0.29	0.97	–	–	–	0.79

finding correlates with the petrographic results previously obtained, i.e., the organic facies are supported by a combination of sapropelite, marine-derived organic matter (alginate and AOM), and small amount of vitrinite derived from land plants (Fig. 3).

In addition, oil-sourcing kerogen types also alter the ‘Ea’ and ‘A’ values. For instance, known Type II-source rocks such as Niobrara, Woodford, Kimmeridge, Mowry, and Madbi shales exhibit a narrow range of Ea between 47 and

56 kcal/mol [46–49]. However, oil-prone source rocks with sulfur-rich kerogen (Type II-S) display a wide range of activation energies varying from 44 to 66 kcal/mol [50, 51].

Based on the kinetic models, our investigated samples exhibit $37 < Ea < 66$ kcal/mol, which are compatible with Type II-S kerogen (Table 2).

Kinetic models also predict geological temperatures and the corresponding vitrinite reflectance (%Ro) values [6, 52, 53]. We assumed the geological heating to be consistent at a

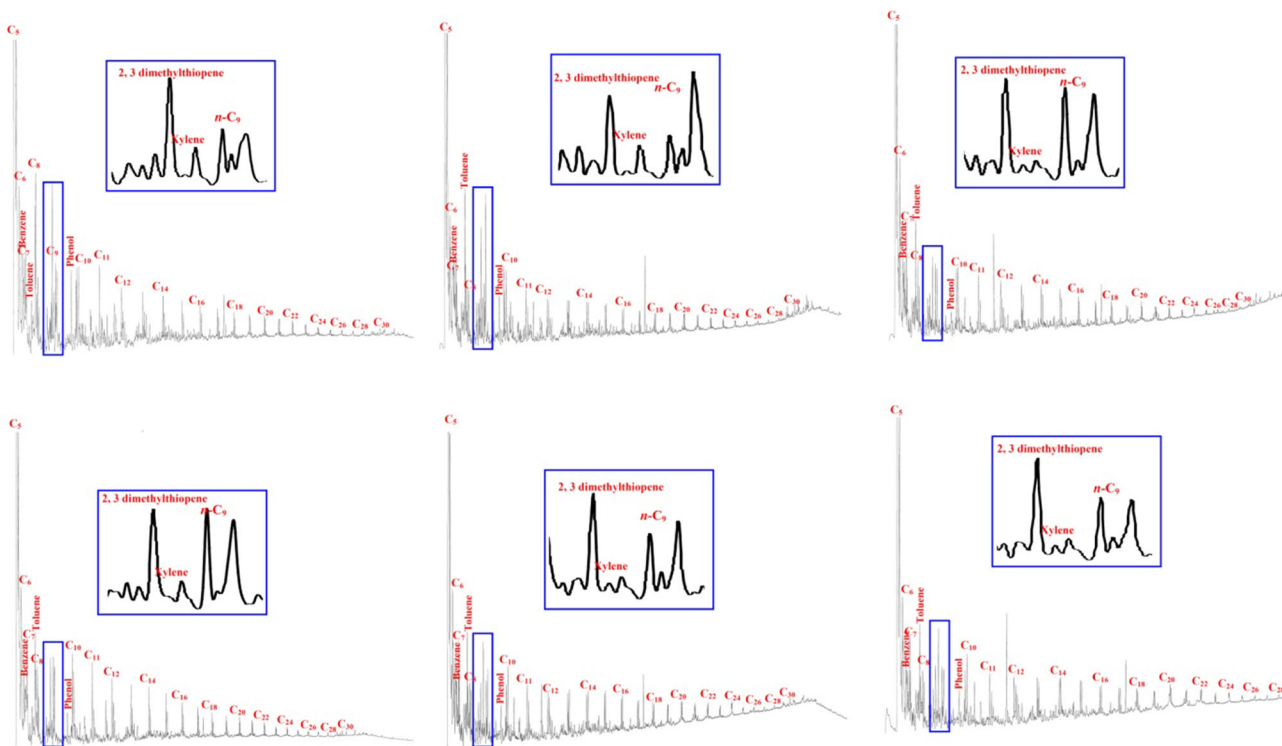


Fig. 5 Py–GC chromatograms of six selected specimens demonstrating the distribution of *n*-alkenes and *n*-alkanes doublets as well as 2,3-dimethylthiophenem toluene, benzene and xylene

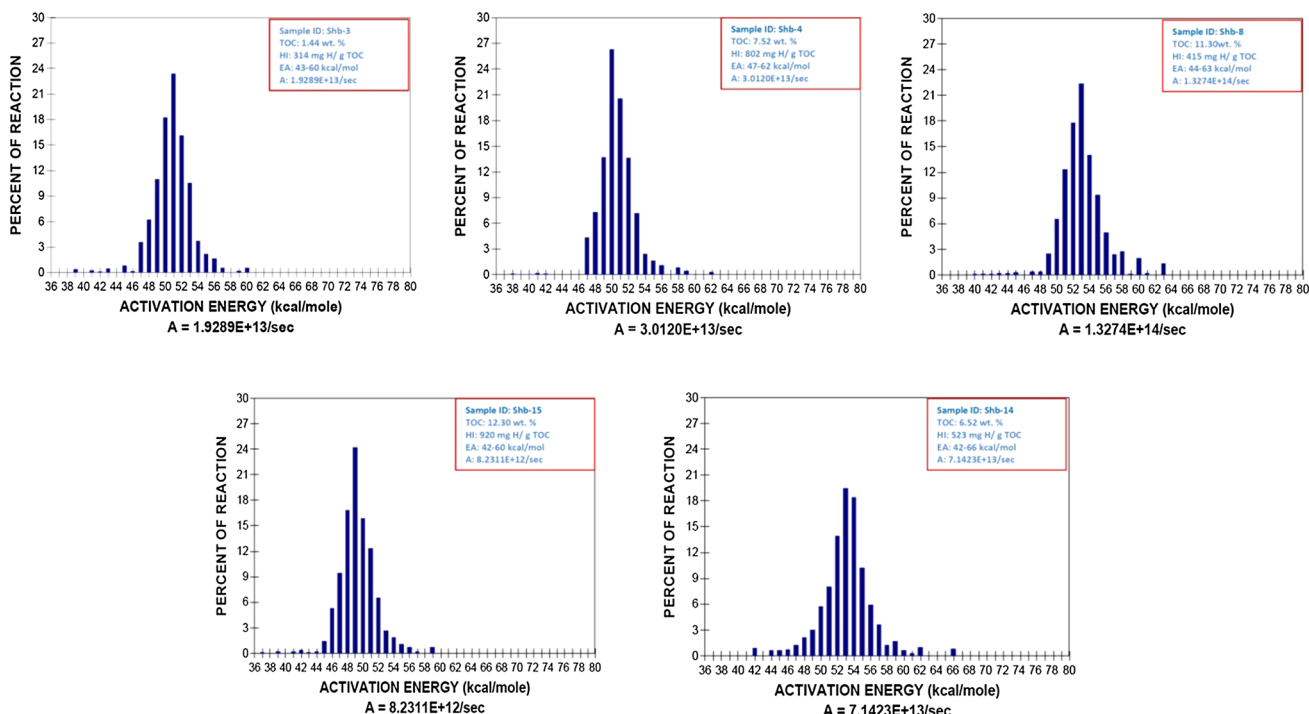


Fig. 6 Distribution of activation energy (Ea) and frequency factors (A) of five specimens exhibiting fairly wide Ea between 42 and 66 kcal/mol, with frequency factors between 8.2311E + 12/sec and 1.3274E + 14/sec.

Data were determined from open system pyrolysis at five heating rates (1 °C, 5 °C, 10 °C, 25 °C and 50 °C/min)

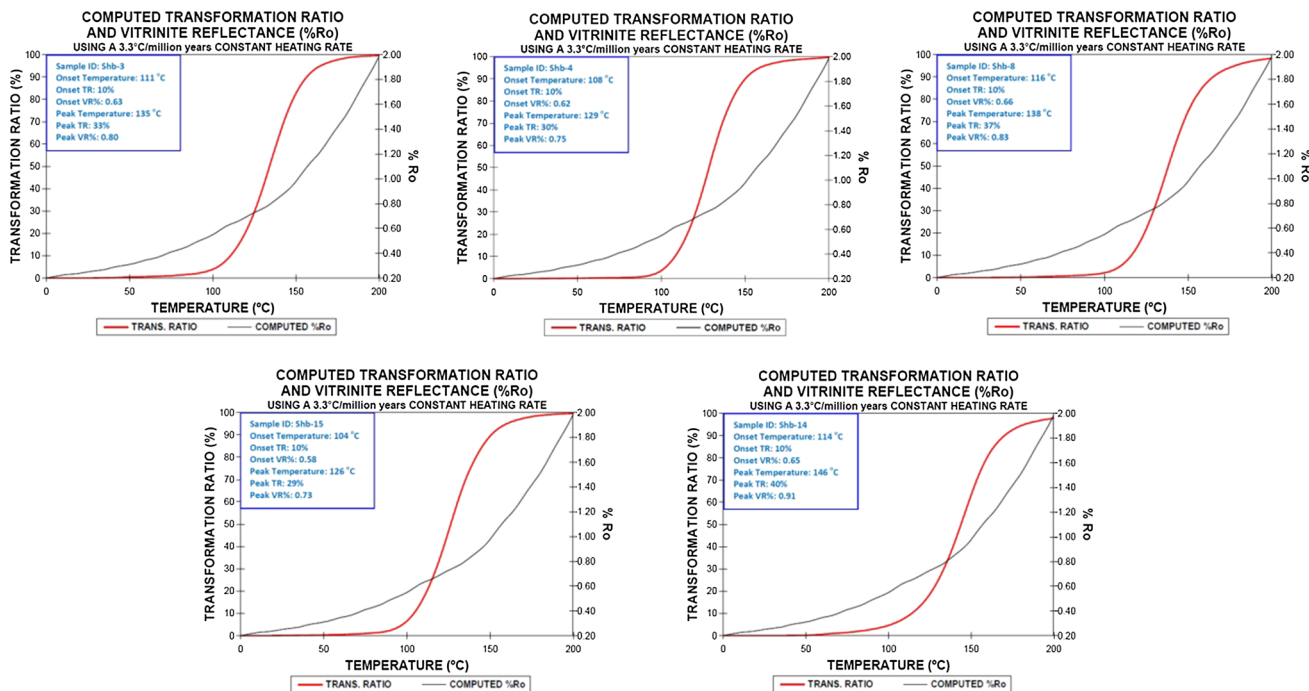


Fig. 7 Kinetic results in terms of computed temperature (°C), TR (TR %) and vitrinite reflectance (VRo) for five specimens exhibiting 104–146 °C temperature, corresponding to computed 0.58–0.91%VRo. Heating rate was assumed constant at 3.3 °C/My

3.3 °C/My rate for kinetic models. The results are presented in Fig. 7, which include calculated transformation ratio (TR)

and VRo. Table 3 shows the bulk kinetic results obtained from this experiment, as well as the expected geological

Table 3 Activation energy, pre-exponential factors (A [1/sec] and predicted onset (TR 10%) and peak generation temperatures, and computed vitrinite reflectance (VR_o) and transformation ratios (TR%) set at a linear heating rate of 3.3 °C/My for five selected organic-rich carbonate rocks within the Upper Cretaceous Shu'ayb Formation from outcrops area in Ajloun area, northern Jordan

Samples ID	TOC (Wt%)	HI (mg/g)	T _{max} (°C)	EA	A factors [1/S]	Computed parameter from kinetics models					
						Onset Temp. (°C)	Peak Temp. (°C)	Onset (Ro %)	Onset (TR %)	Peak (Ro %)	Peak (TR %)
Shb-3	1.44	314	425	39–60	1.9289E + 13/sec	111	135	0.63	10	0.80	33
Shb-4	7.52	802	412	38–62	3.0120E + 13/sec	108	129	0.62	10	0.75	30
Shb-8	11.30	650	415	40–63	1.3274E + 14/sec	116	138	0.66	10	0.83	37
Shb-14	6.52	523	421	37–59	7.1423E + 13/sec	114	146	0.65	10	0.91	40
Shb-15	12.30	920	410	42–66	8.2311E + 12/sec	104	126	0.58	10	0.73	29

TOC total organic carbon, wt%, HI hydrogen index via rock-eval pyrolysis. Tmax temperature at maximum of S2 peak, via rock-eval pyrolysis, EA activation energy distribution via kinetics models, A frequency factor via kinetics models, Onset Temp. (°C) onset (TR 10%) temperature via kinetics models, Peak Temp. (°C) peak generation (geological Tmax) temperature via kinetics models, Peak Temp. (°C) peak generation (geological T_{max}) temperature via kinetics models, Onset (Ro %) computed Onset (Ro %) via kinetics models, Peak (Ro %) computed Peak (Ro %) via kinetics models, Peak (TR) transformation ratio at the peak generation temperature (geological T_{max}) via kinetics models

temperatures at the beginning and peak of petroleum generation. The beginning of the petroleum generation window (% TR) occurs at 104–116 °C, which corresponds to a calculated %VR_o range of 0.58–0.66, according to the observed kinetic models. Type II-S kerogen is reported to exhibit such lower petroleum generation temperature than Types I and II kerogen. The geological temperatures of highest oil generation from the analyzed samples are predicted in the range of 126–146 °C, with corresponding VR_o of 0.73–0.91% (Table 3). The calculated transformation ratios are plotted against the peak generation temperatures (Fig. 11), which shows that the examined samples have a TR of 29–40% between 126 and 146 °C. Therefore, at a geological temperature greater than 146 °C, most of the Type II-S kerogens of the Upper Cretaceous organic-rich carbonates are expected to have been converted into significant amounts of sulfur-rich oil.

5 Discussion

Here, we discuss the geochemical and organic petrological properties and the bulk kinetics results of the organic matter-enriched carbonates from the Late Cretaceous Shu'ayb Formation in the Ajloun area in northern Jordan. These properties are also discussed in order to get insight into their impact on the kind of petroleum that could be formed during thermal maturity and to predict the maximum geological temperatures for petroleum generation. Organic richness and composition are the primary determinants of the quantity and kind of petroleum generated in source rocks [54–56].

Our analyses infer that most of the analyzed carbonate sediments are organically rich and have good to excellent potential to generate petroleum based on the TOC measurements (with highest value reaching 12.30 wt%). A TOC-PY cross-plot indicates that most of the carbonate-rich samples studied had good-to-excellent generative potential (Fig. 8), with PY values as high as 114.46 mg HC/g rock.

Another crucial element in anticipating petroleum generation types is identifying the organofacies (or kerogen typing). The organofacies characteristics and kerogen compositions in the examined organic-rich carbonate samples were principally established by combining the kerogen assemblages from microscope investigations with integrated bulk Rock-Eval and Py-GC pyrolysis data. The Rock-Eval pyrolysis results (i.e., the HI) for the studied samples were typically comparable to those of the organofacies types, indicating that the vast majority of the examined samples had hydrogen-rich Types I and II kerogen and lie within immature zones. In Fig. 9a, this is illustrated by a HI vs. T_{max} cross-plot. This is also supported by the Langford and Blanc-Valleron [57] diagram (i.e., cross-plot between Rock-Eval S₂ and TOC) (Fig. 9b).

Fig. 8 A cross-plot between TOC and PY exhibiting very good–excellent generative capability

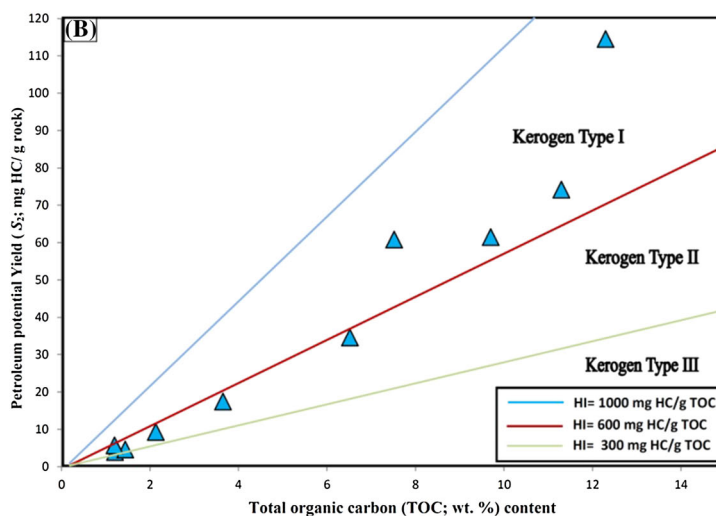
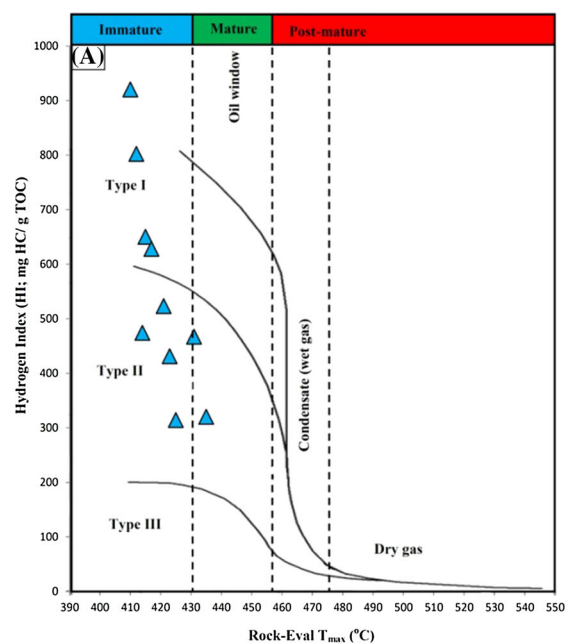
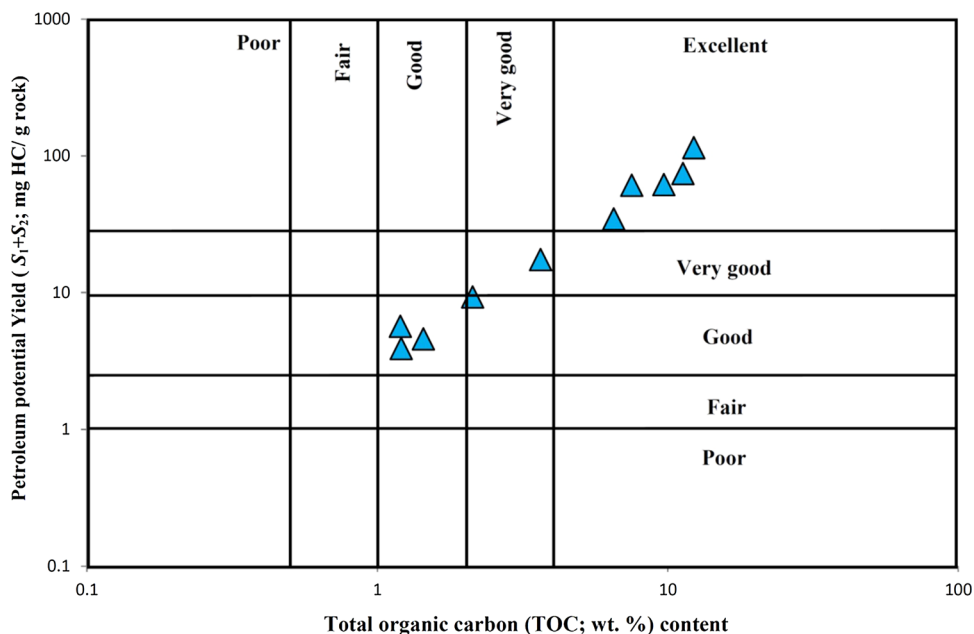


Fig. 9 Kerogen characteristics of the investigated carbonates utilizing **A** a cross-plot between Rock–Eval HI and T_{max} , and **B** TOC vs. Rock–Eval S_2 , showing primarily Types II and II kerogens

The dominance of alginite assemblages (i.e., *telalginite*, *lamalginite*, and *tasmanite*; Fig. 3d–f), and degraded alginites (i.e., AOM fluorescence; Fig. 3c) as well as bituminite and vitrinite phytoclasts (Fig. 3g–k) demonstrate that analyzed samples have a mixture in organic facies [3]. These assemblages imply an anoxic, restricted marine depositional condition [22]. The investigated samples are strongly oil-prone, as shown by the maceral composition and HI- TOC cross-plot (Fig. 10). The significant fraction of fluorescent

liptinites under UV light (Fig. 3b–h) confirms the strong oil-generative potential.

Py–GC data may be used to determine kerogen composition and petroleum-generating facies based on distributions of *n*-alkene and *n*-alkane along with a small abundance of light aromatic hydrocarbons, which implies that the examined carbonate-rich sediments consist of oil-prone kerogen [6, 53]. The same is also supported by the *n*-octane and xylene distributions and their ratios (Fig. 5 and Table 2). This indicates that Type I and II kerogens are the most abun-

Fig. 10 TOC-HI cross-plot exhibiting elevated oil-generative capacity of the investigated organic-rich Upper Cretaceous Shu'ayb carbonates

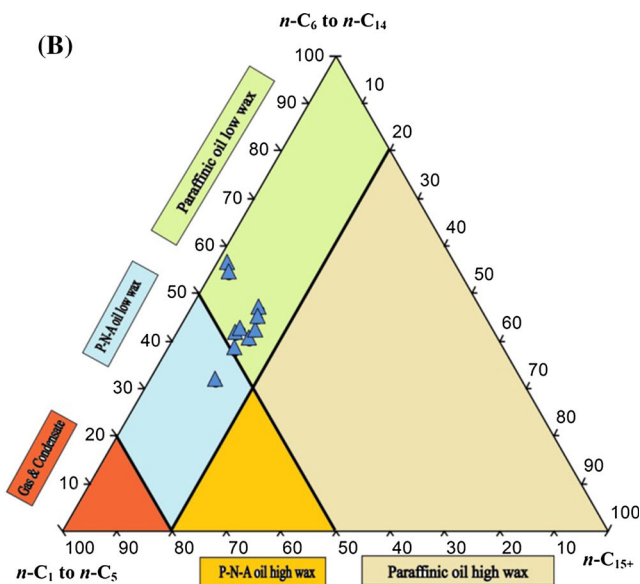
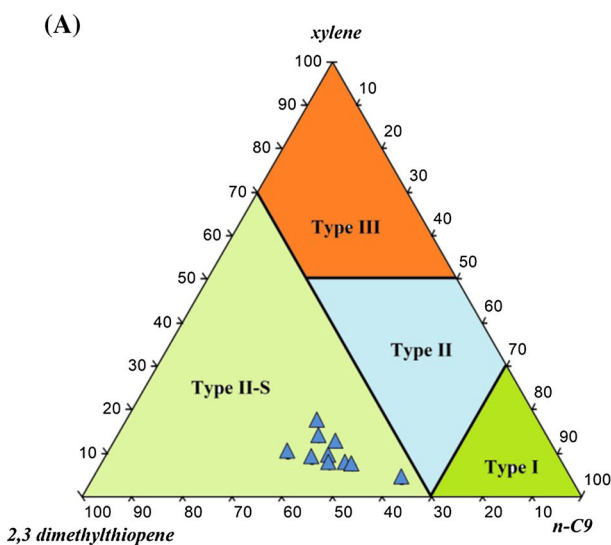
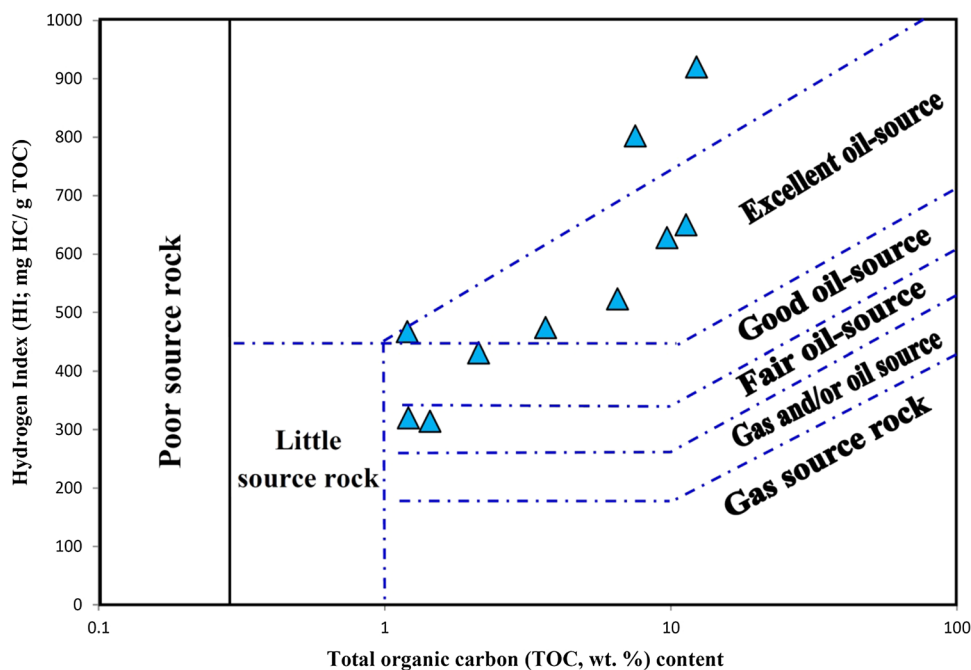


Fig. 11 **A** Ternary diagrams derived from Py–GC data indicating the kerogen type in the analyzed samples using comparative proportions of pyrolyzate components (following Eglinton et al., 1990); **B** the potential hydrocarbon to be generated upon maturation of the Type II-S kerogen

contained in organic-rich carbonates of the Shu'ayb Formation based on the C₁–C₅, the sum total of the C₆–C₁₄, and C₁₅₊; distributions of the *n*-alkene and *n*-alkane exhibiting primarily paraffin oil consisting of little wax

dant organic matters in these sediments, which are capable of producing a substantial volume of oil at appropriate maturity ranges. This type of strong demonstration of kerogen types and petroleum types can be seen in the ternary plots modified by Eglinton et al. [58] and Horsfield et al. [38], where authors utilized the comparative proportions of pyrolyzate components, the amount of C₆–C₁₄, and the C₁₅₊ hydrocarbons of the *n*-alkenes and *n*-alkanes. Results are shown in

Fig. 11A implying the majority of Type II kerogens within the studied specimens to be Type II-S (i.e., rich in sulfur). Therefore, paraffinic oils with minimal wax concentration may have been produced (Fig. 11B).

The wide activation energy ranges of the investigated samples (44–64 kcal/mol; Fig. 6 and Table 2) further corroborate with the existence of Type II-S kerogen (produced from diverse organic matter assemblages). Type II-S kerogen, on

the other hand, may produce oil sooner compared to other oil-sourcing kerogens (Types I/II), correlating to the initial phases of oil-generative window [46].

A VRo range of 0.4–0.8% with 75–135 °C temperature and a heating rate of 3.3 °C/My have been considered for early-oil-generative window. This is supported by the bulk kinetic models of the samples studied. Most of the studied samples attained the beginning (%TR) of bulk petroleum production over relatively low temperatures in the range of 104–116 °C, with corresponding VRo of 0.58–0.66%, according to the kinetic models (Table 3). Peak oil generation is predicted at geological temperatures of 126–146 °C, corresponding to computed VRo of 0.73–0.91% and TR ranging between 29 and 40% (Table 3). Early-mature sulfur-rich oils are expected to have been produced within these low geological temperature ranges, and significant amounts of mature oil will be produced at geological temperatures above 146 °C. These findings are confirmed by the presence of the floating asphalts on the surface of the Dead Sea, as anticipated from early- and heavy-oil generation from Type II-S kerogen [59].

6 Conclusions

The present paper reports the results of integrated geochemical and bulk kinetic investigations of the organic matter-rich carbonate succession within the Upper Cretaceous (Cenomanian–Turonian) Shu'ayb Formation in the Ajloun area of northern Jordan. We concluded the followings:

- The investigated organic matter-rich carbonate sediments in the Shu'ayb Formation exhibit a TOC range of 1.00–12.39 wt%. These primarily comprises Type I and II kerogens (HI = 314–920 HC/g TOC) with high oil-generative potential.
- Py–GC data exhibits high aliphatic compounds, indicating hydrogen-rich kerogens. It also confirms that the examined carbonate-rich sediments are rich in organic sulfur (Type II-S), which may produce high-sulfur oil during the initial phases of the maturity window.
- Kinetic models exhibit a broad activation energy range between 37 and 66 kcal/mol, suggesting Type II-S kerogen types derived from a mixture of organic matter.
- The predicted geological temperatures for the commencement of petroleum generation provide a range of 104 °C–116 °C, which implies that these Type II-S organic facies can start sulfur-rich oil production during the early phases of kerogen cracking.
- The bulk kinetic models reveal that a TR of 29–40% for the Type II-S organic facies occurs at higher temperatures of the petroleum formation over a range of 126–146 °C. Therefore, at geological temperatures exceeding 146 °C,

these organic-rich carbonate deposits are anticipated to represent potential oil source rocks.

Acknowledgements The authors would like to express their gratitude to the Ministry of Science and Higher Education of the Russian Federation under agreement No. 075-15-2022-299 within the framework of the development program for a world-class Research Center “Efficient development of the global liquid hydrocarbon reserves.” The authors extend their sincere appreciation to the Researchers Supporting Project number (RSP-2021/92), King Saud University, Riyadh, Saudi Arabia. The constructive comments by Subject Editor and two anonymous reviewers have improved the original manuscript are gratefully acknowledged.

References

1. Tissot, B.P.; Welte, D.H.: *Petroleum Formation and Occurrence*, 2nd edn., p. 699. Springer Verlag, Berlin (1984)
2. Alali, J.: Jordan oil shale, availability, distribution, and investment opportunity. In: *International conference on oils shale: “Recent Trends in Oil Shale”*, Amman, 7–9 November 2006, Paper No. rtos-A117 (2006)
3. Hakimi, M.H.; Abdullah, W.H.; Alqudah, M.; Makeen, Y.M.; Mustapha, K.A.: Reducing marine and warm climate conditions during the Late Cretaceous, and their influence on organic matter enrichment in the oil shale deposits of North Jordan. *Int. J. Coal Geol.* **165**, 173–189 (2016)
4. Dyni, J.R.: Geology and resources of some world oil-shale deposits. In: *Oil shale developments*, pp. 75–144 (2009)
5. Hakimi, M.H.; Abdullah, W.H.; Alqudah, M.; Makeen, Y.M.; Mustapha, K.A.: Organic geochemical and petrographic characteristics of the oil shales in the Lajjun area, Central Jordan: origin of organic matter input and preservation conditions. *Fuel* **181**, 34–45 (2016)
6. Hakimi, M.H.; Abdullah, W.H.; Alqudah, M.; Makeen, Y.M.; Mustapha, K.A.; Hatem, B.A.: Pyrolysis analyses and bulk kinetic models of the Late Cretaceous oil shales in Jordan and their implications for early mature sulphur-rich oil generation potential. *Mar. Petrol. Geol.* **91**, 764–775 (2018)
7. Hakimi, M.H.; Gharib, A.F.; Alqudah, M.; Ahmed, A.; Hatem, B.A.; Mustapha, K.A.; Zainal Abidin, N.S.; Lashin, A.; Alqubalee, A.M.: Geochemistry and kerogen characteristics of organic-rich chalky marl deposits, northern Jordan: Insights into Type II-S source rock. *Asian. J. Earth Sci.* **225**, 105040 (2021)
8. El-Hasan, T.: Geochemistry of redox-sensitive trace elements and its implication on the mode of formation of the Upper Cretaceous oil shales, Central Jordan. *Njgpa* **249**, 333–344 (2008)
9. Magharbeh, M.; Fayyad, M.; Batarseh, M.: Preparation of natural standard reference material (SRM) for El-lajjun oil shale/Jordan. *Jordan J Earth Environ. Sci.* **4**, 15–22 (2012)
10. Aqleh, S.; van den Boorn, S.; Podlaha, O.G.; Marz, C.; Wagner, T.; Poulton, S.; Kolonic, S.: Reconstruction of redox conditions during deposition of Jordan oil shale using inorganic geochemical records. *Miner. Mag.* **77**, 603 (2013)
11. Ali Hussein, M.; Alqudah, M.; Podlaha, O.: Ichnofabrics of Eocene oil shales from central Jordan and their use for paleoenvironmental reconstructions. *GeoArabia* **19**, 85–112 (2014)
12. März, C.; Wagner, T.; Aqleh, S.; Al-Alaween, M.; van den Boorn, S.; Podlaha, O.G.; Kolonic, S.; Poulton, S.W.; Schnetger, B.; Brum-sack, H.-J.: Repeated enrichment of trace metals and organic carbon on an Eocene high-energy shelf caused by anoxia and reworking. *Geology* **44**, 1011–1014 (2016)



13. Alqudah, M.; Ali Hussein, M.; van den Boorn, S.; Giraldo, V.M.; Kolonic, S.; Podlaha, O.G.; Mutterlose, J.: Eocene oil shales from Jordan—Paleoenvironmental implications from reworked microfossils. *Mar. Petrol. Geol.* **52**, 93–106 (2014)
14. Ali Hussein, M.A.; Alqudah, M.; Blessenohl, M.; Podlaha, O.G.; Mutterlose, J.: Depositional environment of Late Cretaceous to Eocene organic-rich marls from Jordan. *GeoArabia* **20**, 191–210 (2015)
15. Al-Tamimi, M.H.; Alqudah, M.; Al-Atawneh, M.S.; Nazzal, J.; AlShraideh, S.: Depositional environment of Eocene oil shales of Wadi Shallala formation from northern Jordan. *Arab. J. Geosci.* **14**(3), 1–19 (2021)
16. Powell, J.H.; Moh'd, B.K.: Evolution of Cretaceous to Eocene alluvial and carbonate platform sequences in central and south Jordan. *GeoArabia* **16**, 29–82 (2011)
17. Alsharhan, A.S.; Nairn, A.E.M.: *Sedimentary Basins and Petroleum Geology of the Middle East*, p. 843. Elsevier, Amsterdam (1997)
18. Abed, A.: Emergence of Wadi Mujib (Central Jordan) during lower cenomanian time and its regional tectonic implications. *Geol. Soc. Lond. Spec. Publ.* **17**, 213–216 (1984)
19. Schulze, F.; Lewy, Z.; Kuss, J.; Gharaibeh, A.: Cenomanian-Turonian carbonate platform deposits in west central Jordan. *Int. J. Earth Sci.* **92**, 641–660 (2003)
20. Masri, A.: The geology of the Dhiba (Wadi Al-Mujib area map sheet, National mapping project, Bulletin 54 No. 3152-i. Natural Resources Authority, Amman (2003)
21. Al-Rifa'i, I.A.; Cherif, O.H.: Biostratigraphic aspects and regional correlation of some Cenomanian-Turonian exposures in Jordan. *Geol. Mediterr.* **14**, 181–193 (1987). <https://doi.org/10.3406/geolm.1987.1381>
22. Taylor, G.; Teichmüller, M.; Davis, A.; Diessel, C.; Littke, R.; Robert, P.: *Organic Petrology*. Gebrüder Borntraeger, Berlin-Stuttgart, p. 704 (1998)
23. Espitalié, J.; Laporte, J.L.; Madec, M.; Marquis, F.; Leplat, P.; Paulet, J.; Boutefeu, A.: Méthode rapide de caractérisation Des Roches mères, de leur potentiel pétrolier et de leur degré d'évolution. *Rev. Inst. Fr. Petrol.* **32**, 23–42 (1977)
24. Lafargue, E.; Marquis, F.; Pillot, D.: Rock-Eval 6 applications in hydrocarbon exploration, production, and soil contamination studies. *Rev. Inst. Fr. Petrol.* **53**, 421–437 (1998)
25. Espitalie, J.; Deroo, G.; Marquis, F.: La pyrolyse Rock-Eval et ses applications Première partie. *Rev. Inst. Fr. Petrol.* **40**, 563–579 (1985)
26. Peters, K.E.; Cassa, M.R.: Applied source rock geochemistry. *Pet. Syst. Sour. Trap.* 93–120 (1994)
27. Waples, D.W.: Modeling of sedimentary basins and petroleum systems. *Pet. Syst. Sour. Trap.* 307–322 (1994)
28. Larter, S.R.: Application of analytical pyrolysis techniques to kerogen characterization and fossil fuel exploration/exploitation. In: Voorhees, K. (Ed.) *Analytical Pyrolysis*, pp. 212–275. Heinemann, Butterworths, London (1984)
29. Inan, S.; Alp, U.F.; İnan, T.; Yalçın, M.N.; Mann, U.: Relationship between organic matter, sulphur and phosphate contents in upper cretaceous marine carbonates (Karaboğaz Formation, SE Turkey): implications for early oil generation. *J. Pet. Geol.* **33**(4), 319–338 (2010)
30. Schenk, H.J.; Horsfield, B.; Kroos, B.; Schaefer, R.G.; Schwochau, K.: Kinetics of petroleum formation and cracking. In: Welte, D.H.; Horsfield, B.; Baker, D.R. (Eds.) *Petroleum and Basin Evolution*, pp. 231–269. Springer Verlag Heidelberg, Berlin Heidelberg (1997)
31. Burnham, A.K.; Braun, R.L.; Gregg, H.R.; Samoun, A.M.: Comparison of methods for measuring kerogen pyrolysis rates and fitting kinetic parameters. *Energy Fuels* **1**, 452–458 (1987)
32. Burnham, A.K.; Braun, R.L.; Samoun, A.M.: Further comparison of methods for measuring kerogen pyrolysis rates and fitting kinetic parameters. *Org. Geochem.* **13**, 839–845 (1988)
33. McPhilemy, B.: The value of fluorescence microscopy in routine palynofacies analysis: lower carboniferous successions from counties Armagh and Roscommon Ireland. *Rev. Palaeobot. Palynol.* **56**, 345–359 (1988)
34. Tyson, R.V.: *Sedimentary Organic Matter—Organic Facies and Palynofacies*, p. 615. Chapman & Hall, London (1995)
35. Pickel, W.; Kus, J.; Flores, D.; Kalaitzidis, S.; Christanis, K.; Cardott, B.J.; Misz-Kennan, M.; Rodrigues, S.; Hentschel, A.; Hamor-Vido, M.; Crosdale, P.; Wagner, N.: Classification of lip-tinite—ICCP system 1994. *Int. J. Coal Geol.* **169**, 40–61 (2017)
36. Jarvie, D.M.: Total organic carbon (TOC) analysis. In: Merrill, R.K. (Ed.) *Treatise of Petroleum Geology: Handbook of Petroleum Geology, Source and Migration Processes and Evaluation Techniques*, pp. 113–118. American Association of Petroleum Geologists, Tulsa (1991)
37. Katz, B.; Lin, F.: Lacustrine basin unconventional resource plays: Key differences. *Mar. Petrol. Geol.* **56**, 255–265 (2014)
38. Horsfield, B.: Practical criteria for classifying kerogens: some observations from pyrolysis-gas chromatography. *Geochim. Cosmochim. Acta* **53**, 891–901 (1989)
39. Dembicki, H.J.: Improved determination of source quality and kerogen type by combining rock eval and pyrolysis-gas chromatography results (abs.). In: Annual convention programming proceedings 90. AAPG (1993)
40. Dembicki, H.: Three common source rock evaluation errors made by geologists during prospect or play appraisals. *AAPG Bull.* **93**, 341–356 (2009)
41. Dembicki, H.; Horsfield, B.; Ho, T.T.Y.: Source rock evaluation by pyrolysis-gas chromatography. *Am. Assoc. Petrol. Geol. Bull.* **67**, 1094–1103 (1983)
42. Abdullah, W.H.: Oil-generating potential of tertiary coals and other organic-rich sediments of the Nyalau formation, onshore Sarawak. *J. Asian Earth Sci.* **17**, 255–267 (1999)
43. Adegoke, A.K.; Abdullah, W.H.; Hakimi, M.H.: Geochemical and petrographic characterisation of organic matter from the upper cretaceous Fika shale succession in the Chad (Bornu) Basin, north-eastern Nigeria: origin and hydrocarbon generation potential. *Mar. Petrol. Geol.* **61**, 95–110 (2015)
44. Dieckmann, V.: Modelling petroleum formation from heterogeneous source rocks: the influence of frequency factors on activation energy distribution and geological prediction. *Mar. Petrol. Geol.* **22**, 375–390 (2005)
45. Chen, Z.; Liu, X.; Jiang, C.: Quick evaluation of source rock kerogen kinetics using hydrocarbon pyrograms from regular Rock-Eval analysis. *Energy Fuels* **31**, 1832–1841 (2017)
46. Baskin, D.K.; Peters, K.E.: Early generation and characteristics of a Sulfur-Rich Monterey kerogen. *Am. Assoc. Petrol. Geol. Bull.* **76**, 1–13 (1992)
47. Pepper, A.S.; Corvi, P.J.: Simple kinetic models of petroleum formation: part I—oil and gas generation from kerogen. *Mar. Petrol. Geol.* **12**, 291–319 (1995)
48. Jarvie, D.M.; Weldon, W.D.; Leroux, B.; Walker, P.R.: Automated thermal extraction and pyrolysis total petroleum hydrocarbon and kinetic analysis using the SR analyzer. In: Admin. S. pittsburgh conference on analytical chemistry and spectroscopy. Chicago, Illinois, p. 785 (1996)
49. Jarvie, D.M.; Lundell, L.L.: Kerogen type and thermal transformation of organic matter in the Miocene Monterey formation. In: Isaacs, C.M.; Rullkötter, J. (Eds.) *The Monterey Formation: From Rocks to Molecules*, pp. 269–295. Columbia University Press, New York (2001)
50. Behar, F.; Vandenbroucke, M.; Tang, Y.; Marquis, F.; Espitalié, J.: Thermal cracking of kerogen in open and closed systems: determi-



- nation of kinetic parameters and stoichiometric coefficients for oil and gas generation. *Org. Geochem.* **26**, 321–339 (1997)
51. Lewan, M.D.; Ruble, T.E.: Comparison of petroleum generation kinetics by isothermal hydrous and non-isothermal open-system pyrolysis. *Org. Geochem.* **33**, 1457–1475 (2002)
 52. Abbassi, S.; Edwards, D.S.; George, S.C.; Volk, H.; Mahlstedt, N.; di Primio, R.; Horsfield, B.: Petroleum potential and kinetic models for hydrocarbon generation from the upper cretaceous to paleogene latrobe group coals and shales in the gippsland Basin Australia. *Org. Geochem.* **91**, 54–67 (2016)
 53. Makeen, Y.M.; Hakimi, M.H.; Abdullah, W.H.; Mustapha, K.A.; Amir Hassan, M.H.A.; Shushan, I.E.; Garba, T.E.; Abujaish, Y.A.; Lashin, A.A.: Basin modelling and bulk kinetics of heterogeneous organic-rich Nyalau formation sediments of the Sarawak Basin Malaysia. *J. Petrol. Sci. Eng.* **195**, 107595 (2020)
 54. Dow, W.G.: Kerogen studies and geological interpretations. *J. Geochem. Explor.* **7**, 79–99 (1977)
 55. Peters, K.E.: Guidelines for evaluating petroleum source rock using programmed pyrolysis. *Am. Assoc. Petrol. Geol. Bull.* **70**, 318–329 (1986)
 56. Bordenave, M.L.: Screening techniques for source rock evaluation. *Appl. Pet. Geochem.* pp. 217–278 (1993)
 57. Langford, F.F.; Blanc-Valleron, M.M.: Interpreting rock-eval pyrolysis data using graphs of pyrolyzable hydrocarbons vs total organic carbon. *AAPG Bull.* **74**, 799–804 (1990)
 58. Eglinton, T.I.; Sinninghe Damsté, J.S.; Kohnen, M.E.L.; de Leeuw, J.W.: Rapid estimation of the organic sulphur content of kerogens, coals and asphaltenes by pyrolysis–gas chromatography. *Fuel* **69**, 1394–1404 (1990)
 59. Arie Nissenbaum, A.; Aizenshtat, Z.; Goldberg, M.: The floating asphalt blocks of the dead sea. *Phys. Chem. Earth* **12**, 157–161 (1980)

Springer Nature or its licensor holds exclusive rights to this article under a publishing agreement with the author(s) or other rightsholder(s); author self-archiving of the accepted manuscript version of this article is solely governed by the terms of such publishing agreement and applicable law.

